

## Introduction

SESAME is a 2.5 GeV synchrotron radiation facility that has been operating as a user facility since 2016, located in Allan, Jordan. Recently, the storage ring has incorporated a dedicated visible light diagnostics beamline (VDBL) sourced from the 6.5-degree beam port of a bending magnet. Future enhancements for the beamline include the integration of a time-correlated single photon counting unit for measuring the bunch filling pattern, as well as a fast gated camera and a streak camera for longitudinal diagnostics will be done. The beamline has also been extended to operate from outside the tunnel in a dedicated hutch, facilitating more flexible studies, including direct source imaging and double-slit interferometry for beam size measurements and investigations into transverse instabilities

## Beamline Setup

### Old setup

From the outset, the design was intended to be simple and cost-effective. As a result, the system was compactly installed in cell 14 inside the tunnel, positioned vertically in front of the viewport, this setup made calibration and fine focusing more challenging.

### New setup

introduces some adjustments to the layout of the vacuum components inside the tunnel, making it more compact and modifying certain girders. The same in-vacuum mirror water-cooled OFHC copper block, brazed onto a CF63 coated with Al optimized for the visible light range. over 90% reflection efficiency at 500 nm, with  $\lambda/4$  flatness and surface roughness of <20 nm and can handle beam current up to 400 mA.

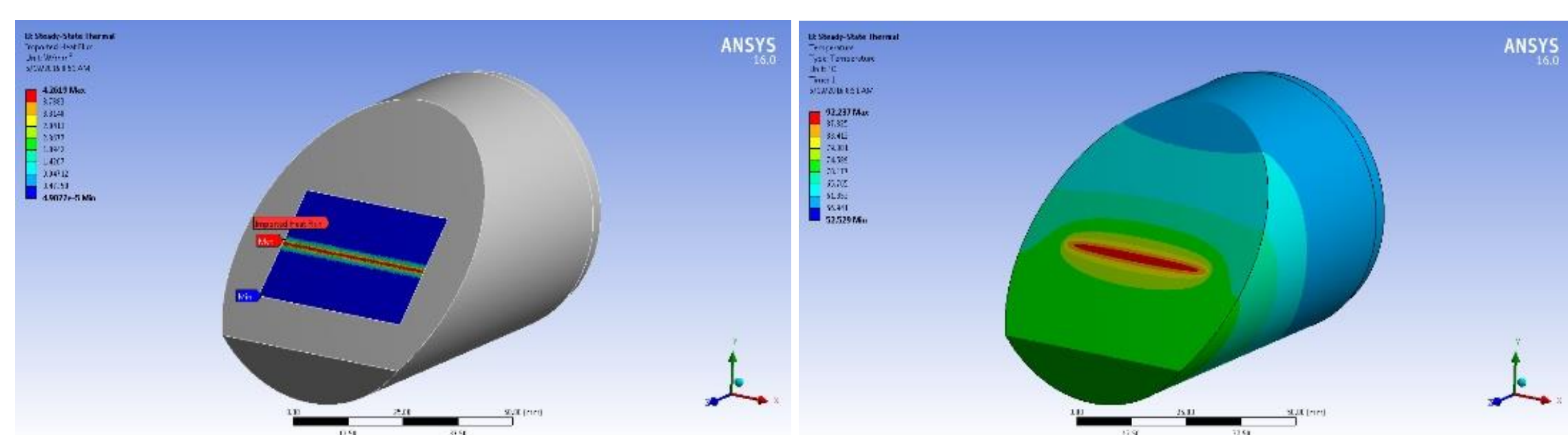


Figure 1: VDBL in-vacuum mirror FEA analyses, power at the mirror (left) temperature distribution (right)

### Layout

The design remains simple, light is extracted by in-vacuum mirror then reflects the light to the hutch through three in-air mirrors. These mirrors are 2-inch circular, flat fused silica mirrors, coated for the visible range and featuring  $\lambda/10$  surface flatness. They are mounted at a 45° angle in kinematic mirror mounts, allowing for precise tip and tilt adjustments using knobs.

Mirror 1 (M1) is positioned 3.7 meters away from the source point and reflects the visible light 90° downward toward Mirror 2 (M2). M2 then reflects the light 90° from the 6.5° beamline port toward the right shielding wall, causing the beam to flip. The shielding wall is 1 meter thick with a 10 cm core opening, positioned 35 cm above the ground. The light then reaches Mirror 3 (M3), followed by Mirror 4 (M4), before arriving at its final destination on the optical table. The total optical path length to the table is approximately 8 meters.

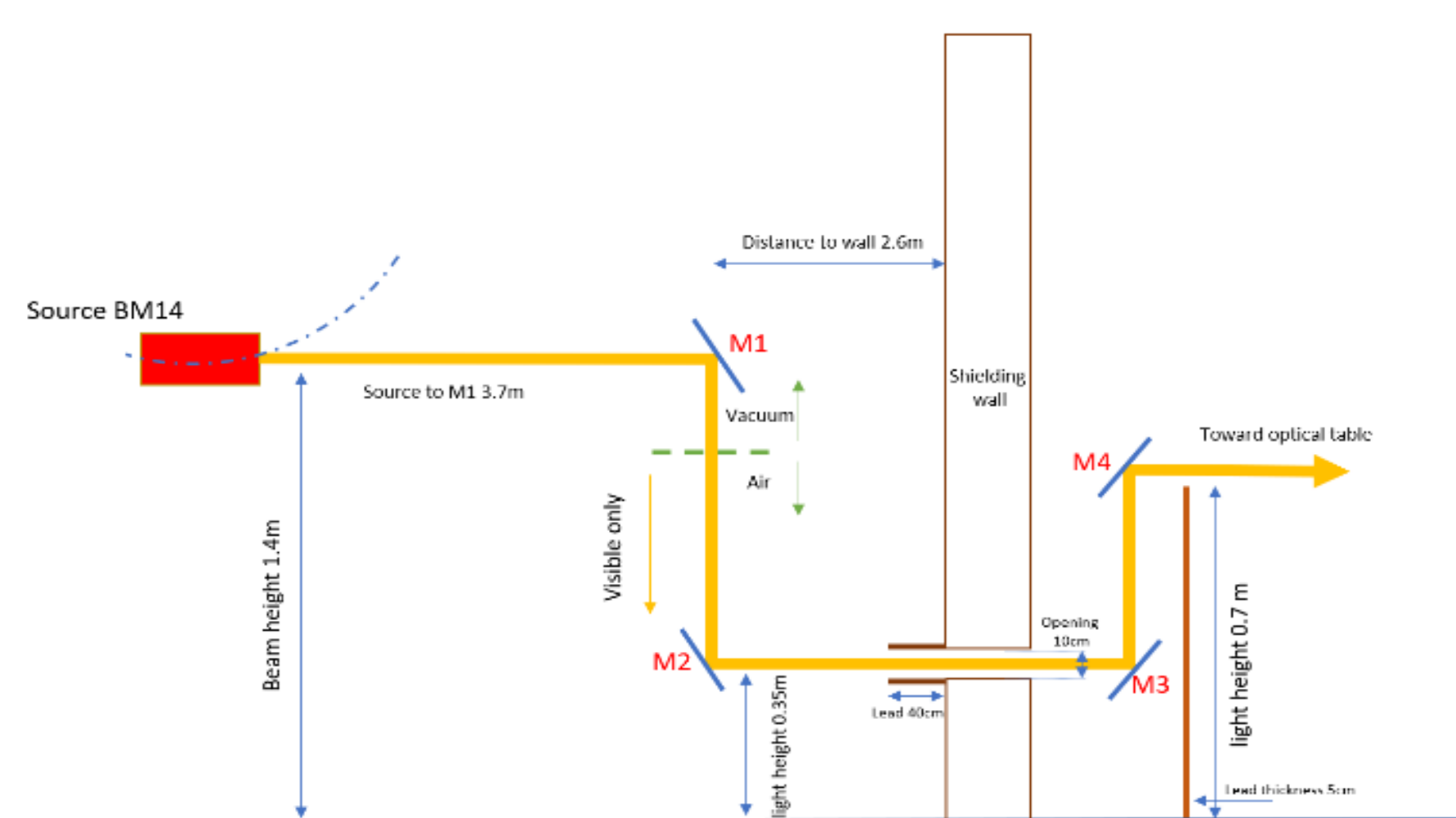


Figure 2: Schematic layout for visible diagnostics beam-line from inside to outside tunnel.

The beamline is situated opposite the transfer line between the booster and the SR. This transfer line contains several fluorescent screens (FS). To make sure the hutch is safe from any potential radiation exposure during various operational modes of the machine, radiation loss studies were conducted using FLUKA. The results indicate that the hutch remains safe under all modes of operation.

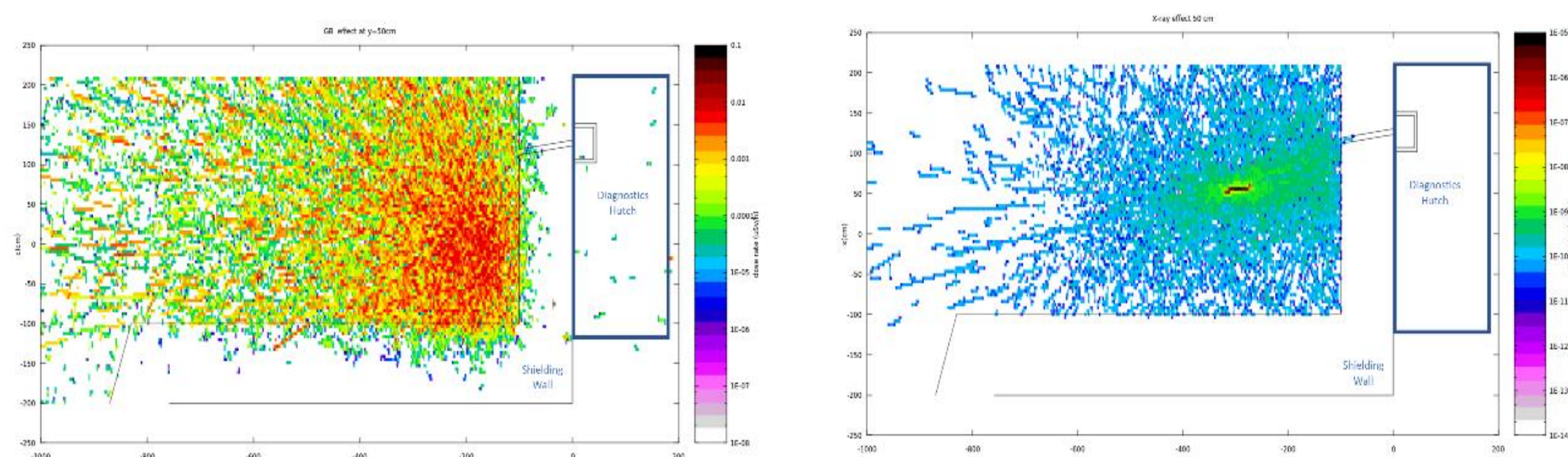


Figure 3: FLUKA simulation, interaction between gas bremsstrahlung-generated inside the bending magnet(left), visualization of the interaction of X-rays with FS in (right).

## Beam Size Measurement Setup

The VDBL includes an imaging system to capture the electron beam profile and a double slit interferometer to measure beam sizes. The interferogram produced by monochromatic and polarized synchrotron light after it passes through a double slit. When these two beamlets are focused onto a CCD camera, the electron beam size can be determined from the visibility of the interferogram, which reflects the complex degree of spatial coherence of the photons. the light distribution that comes out when using slits :

$$I(x) = I_0 \text{sinc}^2\left(\frac{2\pi w}{\lambda d} x + \varphi_s\right) \left[1 + V \cos\left(\frac{2\pi D}{\lambda d} x + \varphi_c\right)\right]$$

where  $I_0$  is the intensity of the interferogram,  $\lambda$  is the light wavelength,  $w$  is the slit width,  $d$  is the distance between the slits and the camera sensor and  $D$  is the separation between slits.  $\varphi_s$  and  $\varphi_c$  are relative phases. And for pinholes :

$$I = I_0 \left\{ \frac{J_1\left(\frac{2\pi a x}{\lambda f}\right)}{\left(\frac{2\pi a x}{\lambda f}\right)} \right\}^2 \times \left\{ 1 + V \cos\left(\frac{2\pi D x}{\lambda f}\right) \right\}$$

where  $a$  is half diameter of the pinhole,  $f$  is the focal distance of the optical system used  $V$  is visibility which is :  $V = \frac{I_{max} - I_{min}}{I_{max} + I_{min}}$

This gives beam size :  $\sigma = \frac{\lambda L}{\pi D} \sqrt{0.5 \ln\left(\frac{1}{V}\right)}$

where  $L$  is the distance between the source point and the double slit system. The double slit system is placed on the optical table, at a distance of 9m from the source point. After passing through a 550nm band pass filter and a linear polarizer, the two light beamlets are focused onto the CCD camera using varifocal objective lens.

**In vertical plane**, the interferogram image of the vertical beam using 4mm separation distance between holes, along with its fitting, is shown in Fig. 4. After fitting the data and applying the equation, a beam size of 81.22  $\mu\text{m}$  was obtained, which is close to the 80.82  $\mu\text{m}$  measured by the pinhole camera, However, the reproducibility of the measurement varied with different settings. VDBL is significantly affected by Fraunhofer diffraction. As a result, the intensity of the radiation at the position of the double slit is unequal between the two slits, and this intensity imbalance must be considered To improve the accuracy of beam size measurements using the interferometer technique, an alternative approach involves scanning the distance between the pinholes,  $D$ , resorting equation gives:

$$V = e^{-2\pi \frac{\sigma^2 D^2}{\lambda^2 L^2}}$$

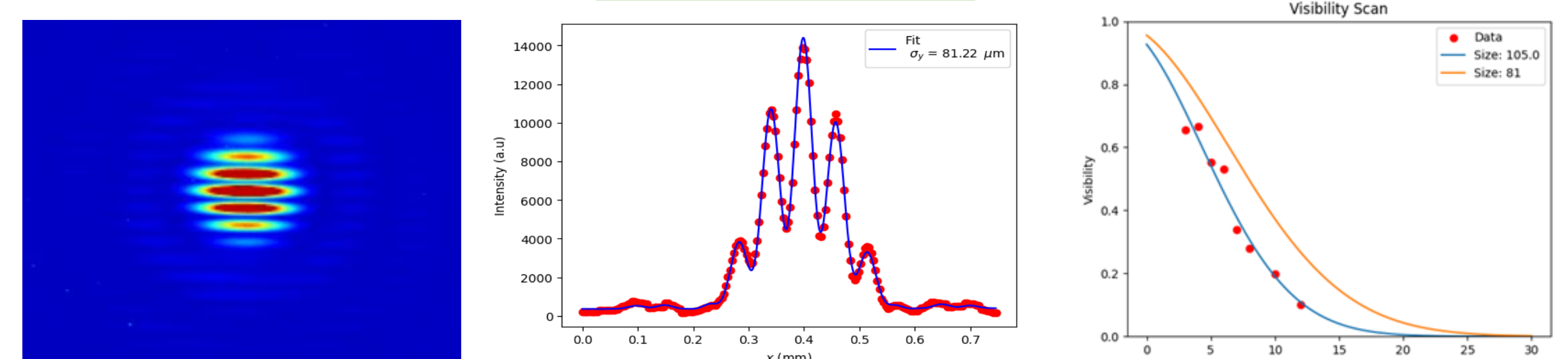


Figure 6: Vertical interferogram image (left) with fitting using 4mm slit separation (middle) and visibility as a function of the distance between pinholes (right)

**In horizontal plane**, several measurements were conducted using different slit separations. For each separation distance  $D$ , multiple data acquisitions were performed. The initial results showed good agreement with the theoretical value of the horizontal beam size, as well as with measurements from the pinhole camera ( $\sim 232 \mu\text{m}$ ).

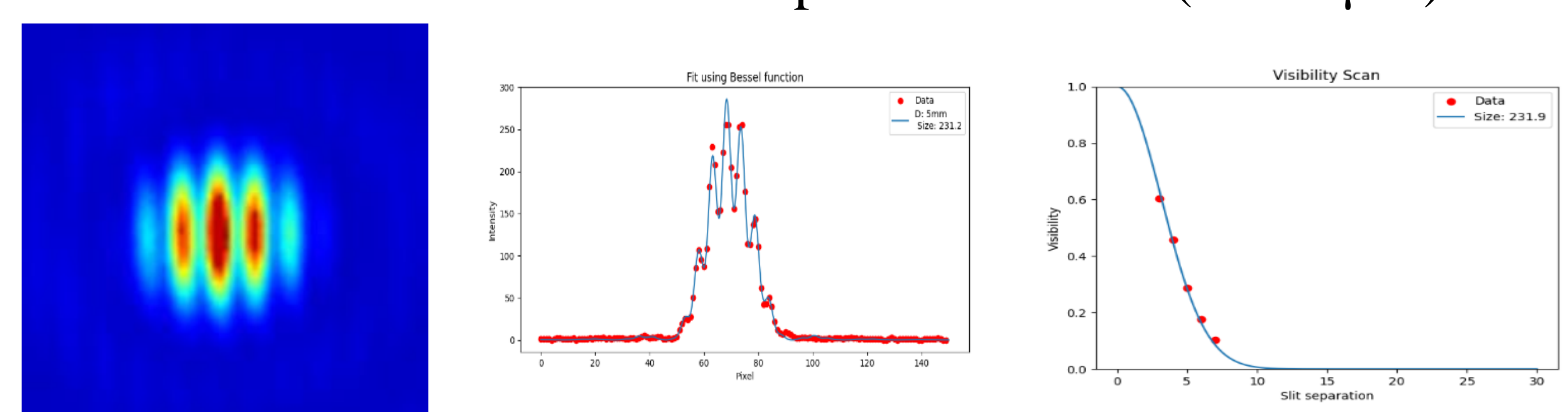


Figure 7: Horizontal interferogram image (left) with fitting using 5mm slit separation (middle) and visibility as a function of the distance between pinholes (right)